

The Regioselectivity of Internal Hydrogen Abstraction by Triplet *o*-*tert*-Amylbenzophenone

Peter J. Wagner,* Raul Pabon, Bong-Ser Park, Ali R. Zand, and Donald L. Ward

Contribution from the Chemistry Department, Michigan State University, East Lansing, Michigan 48824

Received October 1, 1993. Revised Manuscript Received November 26, 1993*

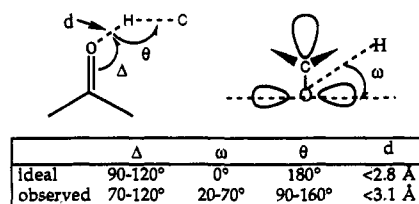
Abstract: The title ketone undergoes triplet-state δ -hydrogen abstraction to produce two diastereomeric sets of 1-phenyl-1-indanols: the 2,3,3-trimethyl isomers **2Z** and **2E** by abstraction of a methylene hydrogen and the 3-methyl 3-ethyl isomers **1Z** and **1E** by abstraction of a methyl hydrogen. The **2**/**1** ratio varies only modestly with changes in solvent, temperature, and phase, ranging from 0.7 in hydrocarbons to 1.6 in methanol, 2.4 in the crystal, and 3.5 on silica. Total quantum yields are 0.034 in benzene and 0.43 in methanol. After correction for reversion of the intermediate 1,5-biradicals to the ketone, the product ratios indicate a 1/1.6 ratio for abstraction of secondary *versus* primary hydrogens in solution and a $\leq 7/1$ ratio in the solid. X-ray analysis and conformational modeling indicate a high steric energy for the compound, with only a few conformations populated even in solution. The favored orientations of the methyl and methylene hydrogens with respect to the carbonyl oxygen are significantly different, with the former lying at positions that are predicted to be of low reactivity. Molecular flexibility might alter these geometries, but the low (2.5 kcal/mol) activation energy for hydrogen abstraction suggests that the geometries of the transition states for hydrogen abstraction cannot deviate significantly from those of the conformational minima of the triplet reactant. Whereas there is no *Z/E* diastereoselectivity in solution, both *Z* isomers are favored by 3-4/1 in the solid. Least-motion cyclization of the biradicals from their initial geometries explains the preference for *Z* products. These results suggest a lack of stringent stereoelectronic requirements for hydrogen abstraction.

A few years ago, we reported that *o*-*tert*-butylbenzophenone (otBBP) undergoes a highly efficient Yang photocyclization reaction to produce 3,3-dimethyl-1-phenyl-1-indanol.¹ The reaction proceeds *via* very rapid ($k_{295^\circ} \approx 10^9 \text{ s}^{-1}$) hydrogen abstraction by the n, π^* triplet to form a 1,5-biradical that either cyclizes to the indanol or disproportionates back to the starting ketone. The biradical's lifetime and its partitioning both are strongly solvent dependent, with the longest lifetime and the highest indanol quantum yield occurring in methanol, the shortest lifetime and lowest quantum yield in hydrocarbon solvents. The extremely high rate constant and the low activation energy (2.5 kcal/mol) for abstraction of a primary hydrogen are unusual and have been interpreted as reflecting some relief of steric congestion in this crowded molecule.²

otBBP has two separate methyl hydrogens within 2.7 Å of the carbonyl oxygen. The fact that otBBP reacts in the solid as well as in solution introduces the question of whether one or both hydrogens react. These hydrogens are positioned at much different orientations with respect to the carbonyl orbitals of the triplet ketone; H_A makes a dihedral angle, ω , of 40° with the long axis of the half-occupied oxygen n orbital, whereas H_B is nearly perpendicular to that axis. It makes no difference which methyl group reacts in solution, since rapid bond rotation interconverts the two biradical conformations. However, bond rotation may not be so facile in the crystal, and the biradical formed by abstraction of H_A may not be able to rotate into the geometry required for cyclization.³ The biradical formed by abstraction of H_B has a geometry suitable for cyclization; so, the solid-state reaction conceivably could prefer this route.

Scheffer has described the geometric factors that should influence hydrogen abstraction reactivity by n, π^* triplets;⁴ they are depicted in Chart 1. Of these, the effect of ω values on reactivity has become a question of intense interest, ω being the

Chart 1



dihedral angle made by the hydrogen atom with respect to the nodal plane of the carbonyl π bond. Several theoretical analyses have predicted vanishing reactivity when $\omega = 90^\circ$,⁵ and some experiments indicate lowered rate constants at high values of ω .⁶⁻⁸ Such considerations would suggest that H_A should react with a higher rate constant than H_B . The predicted requirement that $\theta \gg 90^\circ$ is reflected in the large calculated enthalpic preference for 1,5- and 1,6- over 1,4-H transfers.⁹ Actual values observed in solid-state photochemistry deviate greatly from the theoretical values.⁴

This paper reports our efforts at measuring the relative reactivities of H_A and H_B . An unsymmetrical *tert*-alkyl group is required for this purpose; we chose *o*-*tert*-amylbenzophenone (otAmBP), hoping that its ethyl group would preferentially occupy the position carrying H_A in the most stable conformation as well as in the crystal. These expectations were verified; H_A and H_B (now H_2 and H_1 , respectively) were found to react with similar efficiency in both the solid and in solution.

(5) Severance, D.; Pandey, B.; Morrison, H. *J. Am. Chem. Soc.*, **1987**, *109*, 3231. Severance, D.; Morrison, H. *Chem. Phys. Lett.* **1989**, *163*, 545. Dorigo, A. E.; McCarrick, M. A.; Loncharich, R. J.; Houk, K. N. *J. Am. Chem. Soc.* **1990**, *112*, 7508.

(6) Sugiyama, N.; Nishio, T.; Yamada, K.; Aoyama, H. *Bull. Chem. Soc. Jpn.* **1970**, *43*, 1879. Colpa, J. P.; Stehlik, D. *J. Chem. Phys.* **1983**, *81*, 163. Sauer, R. R.; Scimone, A.; Shams, H. *J. Org. Chem.* **1988**, *53*, 6084. Sauer, R. R.; Krogh-Jespersen, K. *Tetrahedron Lett.* **1989**, *30*, 527.

(7) Ito, Y.; Matsuura, T.; Fukuyama, K. *Tetrahedron Lett.*, **1988**, *29*, 3087.

(8) Wagner, P. J.; Zhou, B.; Hasegawa, T.; Ward, D. L. *J. Am. Chem. Soc.* **1991**, *113*, 9640.

(9) Dorigo, A. E.; Houk, K. N. *J. Am. Chem. Soc.* **1987**, *109*, 2195.

* Abstract published in *Advance ACS Abstracts*, January 1, 1994.
(1) Wagner, P. J.; Giri, B. P.; Scaiano, J. C.; Ward, D. L.; Gabe, E.; Lee, F. L. *J. Am. Chem. Soc.* **1985**, *107*, 5483.

(2) Wagner, P. J.; Pabon, R.; Cao, Q. *J. Am. Chem. Soc.* **1992**, *114*, 347.

(3) Appel, W. K.; Jiang, Z. Q.; Scheffer, J. R.; Walsh, L. *J. Am. Chem. Soc.* **1983**, *105*, 5354.

(4) Scheffer, J. R. *Org. Photochem.* **1987**, *8*, 249.

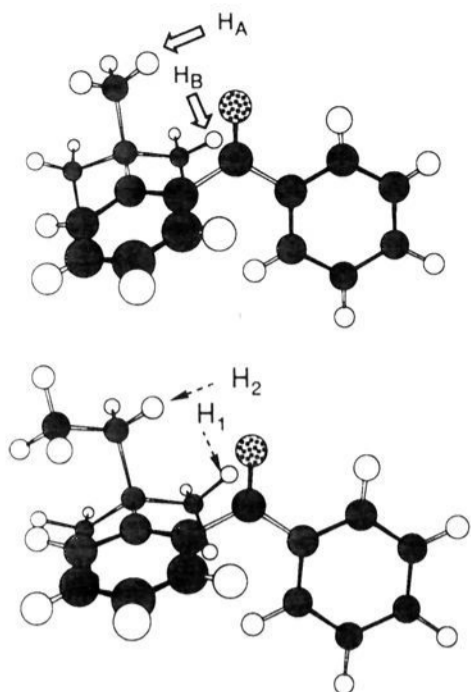


Figure 1. X-ray crystal structures of otBBP (top) and otAmBP (bottom).

Scheme 1

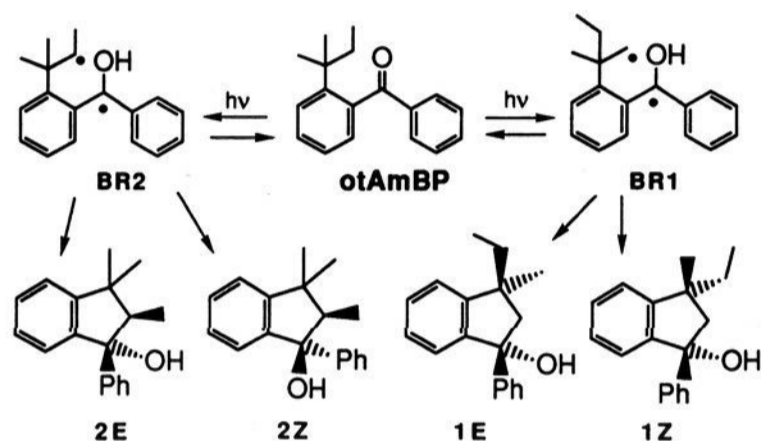
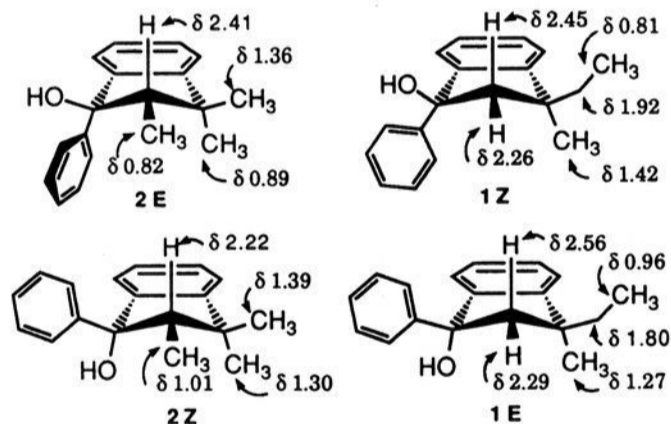


Chart 2



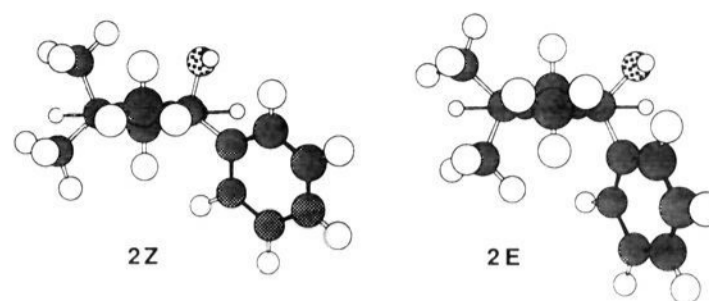
Results

Synthesis. otAmBP was synthesized uneventfully from *tert*-amylbenzene by the reported process for *o*-bromo-*tert*-butylbenzene: nitration, removal of the ortho isomer, bromination, reduction of nitro, and reduction of the diazonium salt.¹⁰ Its Grignard reagent was reacted with ethyl benzoate to provide otAmBP.

Product Identification. Preparative scale irradiation of dilute ketone in benzene produced four indanol photoproducts, which were separated by semipreparative HPLC. They were identified by their ¹H-NMR spectra and used to calibrate the HPLC for quantitative analysis.

Chart 2 presents the NMR evidence most germane in distinguishing diastereomeric relationships in the two pairs of indanols. Although it is not necessary to distinguish between diastereomers for the purpose of determining total 2/1 ratios, understanding stereoselectivity required the effort. The difference between chemical shifts of the 2-methyl groups was used to

Chart 3



distinguish 2E and 2Z, since a *cis*-phenyl is known to shield an adjoining methyl in several cyclopentanol derivatives. NOE experiments confirmed these assignments; irradiation of the δ 0.82 2-methyl doublet in 2E enhanced some 1-phenyl resonances, whereas comparable irradiation of the δ 1.01 2-methyl doublet in 2Z did not. It is assumed that the five-membered ring prefers to be puckered, with the largest substituents at carbons 1 and 3 pseudoequatorial. The *E* isomer apparently prefers the conformation shown, with the phenyl pseudoaxial and the 2-methyl equatorial. This is the only geometry that would strongly shield both the 2- and 3-methyl groups. It is well known that axial phenyl rings on cyclohexane twist to avoid nonbonded interactions between their ortho hydrogens and the syn axial substituents.¹² In the case of a puckered cyclopentane, such a twist would also avoid steric interaction with the 2-methyl group. Molecular mechanics computations suggest that the phenyl(ax)-methyl(eq) conformer is 1.8 kcal/mol more stable than the phenyl(eq)-methyl(ax) conformer. Thus, we feel confident in our assignments of 2E and 2Z, as depicted by the energy minimized structures in Chart 3.

The spectra of 1E and 1Z are very similar. Shift reagents were not useful in differentiating the two, presumably because complexation with the tertiary alcohols is sterically inhibited, but did cause significant dehydration of the alcohols. NOE experiments were performed on a mixture of 1E and 1Z by separate irradiation of the 3-methyl resonances. In the isomer with the δ 1.27 3-methyl singlet, enhancement of a single aryl proton (the one at δ 7.07) occurs. The other isomer was concluded to be Z, with the methyl and phenyl groups *cis*, since several of the aryl protons were enhanced in the NOE experiment. This 1Z apparently exists in two conformations, with the 3-methyl group being deshielded by the fused benzene ring in one conformation and being close to some 1-phenyl protons in the conformation shown. Since no shielding of the 3-methyl occurs in 1Z comparable to that observed in 2E, we conclude that the 1-phenyl is not twisted in 1Z as it is in 2E because of the absence of a 2-methyl group; AM1 calculations lend support to this view.

Figure 2 shows the NMR spectrum of an otAmBP sample in benzene-*d*₆ irradiated until all starting ketone had disappeared; all four products could be clearly distinguished in the mixture. Their NMR ratios confirmed those measured by HPLC. GC analysis caused significant dehydration; simple vacuum solvent removal or preparative HPLC caused minor dehydration for all but 2Z. The two indenes were easily identified by their NMR spectra. One fully irradiated sample in benzene was treated with HCl; GC analysis showed only two peaks, assigned to the indenes, corresponding to the 3:2 1/2 ratios observed by HPLC and NMR.

Product ratios were determined by both NMR integration and HPLC analysis, as just described. Table 1 lists the values measured in several solvents and under a variety of conditions. In all cases, product ratios were independent of conversion. As with otBBP, reaction proceeded at low temperatures and in the solid as well as in solution. In the case of crystalline otAmBP, a large crystal held in a constricted test tube was irradiated briefly. The crystal was then quickly washed with a few drops of methanol

(10) Crawford, M.; Stewart, F. H. C. *J. Chem. Soc.* 1952, 4441.

(11) Wagner, P. J.; Meador, M. A.; Zhou, B.; Park, B.-S. *J. Am. Chem. Soc.* 1991, 113, 9630.

(12) Allinger, N. L.; Tribble, M. T. *Tetrahedron Lett.* 1971, 3259.

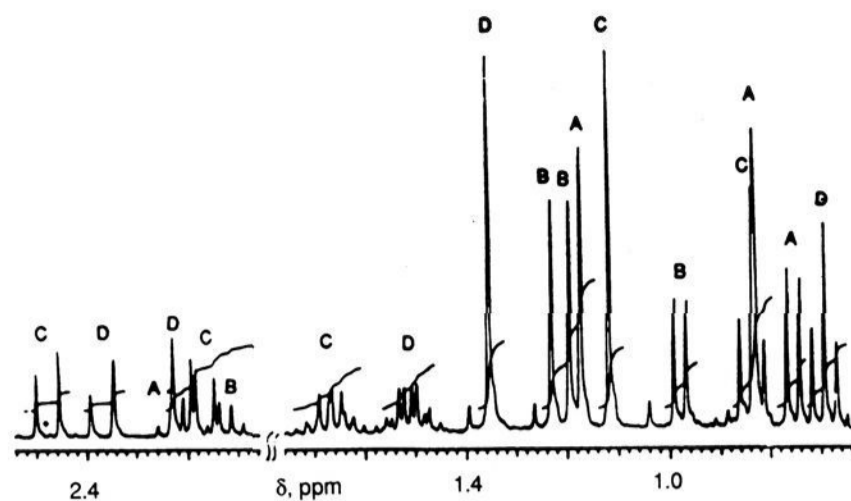


Figure 2. High-field region of the NMR spectrum of a fully irradiated sample of otAmBP, 0.01 M in benzene- d_6 : A = 2E, B = 2Z, C = 1E; and D = 1Z.

Table 1. Product Distribution obtained upon Irradiation of otAmBP

reaction medium	irradiation temperature	percentages of each product			
		2E	2Z	1Z	1E
benzene	ambient	20	20	30	30
toluene	-78 °C	10	10	40	40
dioxane	ambient	27	20	32	21
acetonitrile	ambient	27	25	25	23
methanol	ambient	34	28	24	14
methanol ^a	70 °C	35	28	24	13
methanol ^a	-78 °C	35	28	24	13
methanol ^b	77 K	12	48	33	7
crystal	ambient	17	54	21	8
silica gel	ambient	26	52	11	11

^a 10% ethanol. ^b 50% ethanol.

three times in succession. The product ratio was identical within experimental error in all three washings, although the last two washings gave successively lower yields of products. The silica sample was prepared by adding 200 mesh silica gel to a methylene chloride solution of otAmBP. After the solvent had been evaporated, the loaded silica was packed into a melting point capillary tube. After irradiation, the tube was broken and the organics were extracted into an NMR solvent.

Quantum efficiencies were measured by irradiating dilute otAmBP solutions in parallel with valerophenone ($\Phi = 0.33$) or *o*-methylvalerophenone solutions ($\Phi = 0.016$).¹³ Product yields were measured by HPLC and converted to the following quantum yields: 0.034 in benzene and 0.43 in methanol.

Flash Kinetics. Identical studies to those reported for otBBP¹ were conducted. Dilute otAmBP in methanol at 20° was excited with a 308-nm excimer laser (4-ns pulse) and monitored at 370 nm where the short-lived triplet does not absorb strongly but the 1,5-biradical does. A biphasic decay was observed; it consisted of two components of comparable initial intensities with lifetimes of ~25 and ~45 ns. No attempt was made to analyze the decays more quantitatively, since the important conclusion is that otAmBP produces two different biradicals in comparable amounts.

Structure of otAmBP. Figure 1 compares the crystal structure of otAmBP with that of otBBP. Apart from a slight twist of the *tert*-amyl group, the two structures are nearly identical. Most important, hydrogens H₁ and H₂ occupy nearly the same positions in space with respect to the carbonyl group as do H_A and H_B in otBBP: $d(\text{O}-\text{H}_2) = 2.63 \text{ \AA}$, $\omega = 45^\circ$; $d(\text{O}-\text{H}_1) = 2.53 \text{ \AA}$, $\omega = 95^\circ$. Thus, our hopes that the primary and secondary hydrogens in otAmBP would adopt unique positions in the crystal were largely realized. The thermal anisotropic factor *B* for the methyl fragment of the ethyl group was rather large compared to those of the other carbons; analysis of excess electron density indicated the possible presence of no more than 15% of the conformer in which the *tert*-amyl group is twisted 120°. The positions of all other carbons appear to be singular.

(13) Wagner, P. J.; Chen, C.-P. *J. Am. Chem. Soc.* 1976, 98, 239.

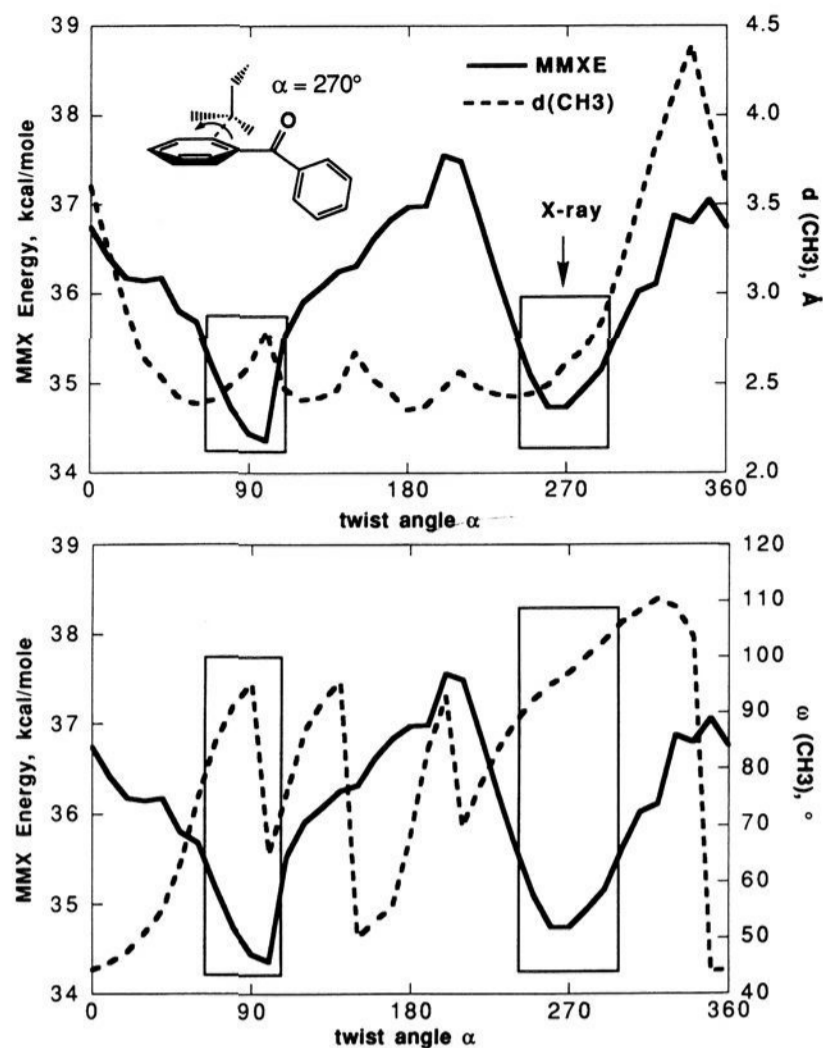
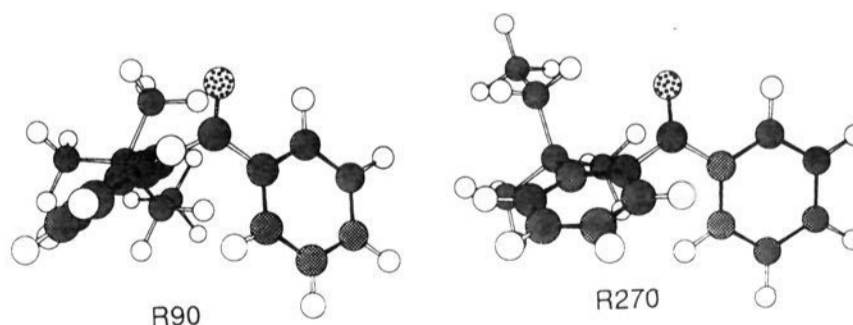


Figure 3. Comparisons of calculated (MMX) energies (—) of otAmBP with (top) *d* values and (bottom) ω values (---) as a function of rotation around the benzene-*tert*-amyl bond.

In order to estimate the distribution of different conformations in solution, we performed various calculations on otAmBP, using a dihedral driver for rotation around the benzene-*tert*-amyl bond. These efforts revealed two energy minima, separated by a barrier of 2.5-3 kcal/mol, in both of which the ethyl group is held perpendicular to the benzene ring. One of these conformers (R270) closely resembles the crystal structure, except for a 120° twist of the ethyl group. The other (R90) is related by a 180° rotation of the *tert*-amyl group. MMX computes R90 to be more stable than R270 by only 0.3 kcal/mol; MM2 places R270 0.2 kcal below R90. AM1 geometry optimizations were performed with the *tert*-amyl rotation frozen; the minimized R90 and R270 geometries were computed to have the same energy within 0.05 kcal. MM2 indicates that R270 is only 0.12 kcal/mol more stable than the X-ray geometry R270x. The possible minor conformation in the crystal represents a geometry, R30, between R270 and R90.



Structure R90 has no ethyl but two methyl hydrogens within 2.7 Å of the oxygen; their positions are described by angles ω of 65° and 99° and angles θ of 90° and 110°, respectively. The distances, but not the angles, are very sensitive to rotation; a change of 25° in either direction moves one hydrogen to $d > 3 \text{ \AA}$, which is too far for reaction to occur.⁴ A rotation of 60° brings one hydrogen very close to the oxygen such that θ improves to 140°; MM2 calculations indicate a 4 kcal/mol barrier to this rotation. Figure 3 plots the calculated MMX energies as a

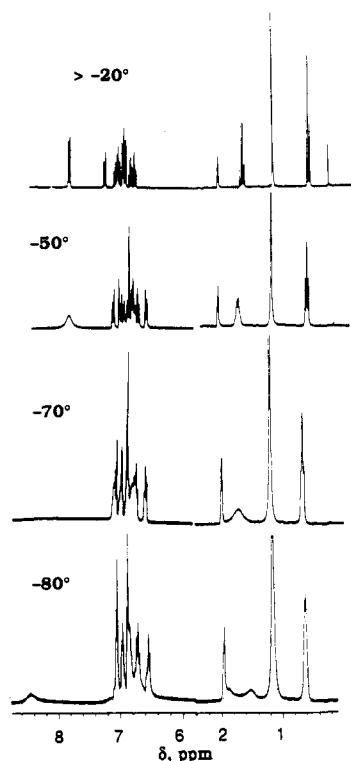
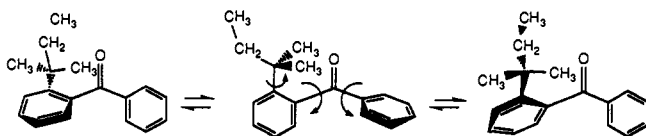


Figure 4. Temperature dependence of the NMR spectrum of otAmBP in toluene- d_8 .

Scheme 2



function of twist angle and correlates them independently with d and ω values at each geometry.

Low-temperature NMR studies are consistent with the low calculated barrier to rotation of the *tert*-amyl group. The spectrum of otBBP shows no line broadening down to -80° . However, the coupled rotations of the carbonyl–benzene bonds in otAmBP freeze out at -70° . (MM2 calculations predict a 9 kcal/mol barrier.) The resonances of the two ortho hydrogens on the benzoyl group coalesce at -70° and separate into peaks 1.3 ppm apart, with the upfield peak at δ 7.1 being partially obscured by other aromatic signals. The two methylene protons become nonequivalent at the same time, as shown in Figure 4. The same effects are also observed in CH_2Cl_2 , where the two methyl groups become nonequivalent below -85° . The *tert*-amyl constituents exchange positions *via* 180° rotations of both the *tert*-amyl group and the benzoyl bonds. Such coupled rotation of the benzene rings seems to be hindered by the *tert*-amyl more than by a *tert*-butyl group.

Since it is well known that $\text{C}=\text{O}$ bonds are longer in the n,π^* triplet than in the ground state,¹⁴ we performed two additional calculations of barriers to rotation of the *tert*-amyl group. In one case, a MM2 computation was done on the ground state with the $\text{C}=\text{O}$ bond locked at 1.5 Å. In another, a triplet UHF AM1 computation was carried out. Both methods reproduced the barrier of 2.0–2.5 kcal/mol found for the simple ground state, with a maximum when the ethyl group lies in the plane of the benzene ring, as shown in Figure 3.

Discussion

The primary motivation for this study was to acquire evidence regarding the orbital orientational requirements for hydrogen-atom abstraction by triplet carbonyls. We shall consider our results first from a qualitative perspective and then provide more quantitative analyses.

The X-ray crystal structure of otAmBP shown in Figure 1 compares very favorably with one (R270) of two conformational minima calculated by both molecular mechanics and AM1, the only difference being the positioning of the methyl fragment of the ethyl group. It is twisted 120° in the crystal relative to its lowest energy form. Inspection of the unit cell reveals that this geometry allows tighter packing than does R270. Careful analysis of excess electron density indicated no likelihood of any significant population of either R270 or R90 in the crystal. Fortunately for this study, both the X-ray and R270 geometries have one of the two secondary hydrogens in identical positions (H_2) with respect to the carbonyl. The very small calculated energy difference between the X-ray and R270 conformations means that the two are equally populated in solution and can be considered as one; we shall refer to the X-ray geometry as R270x.

Figure 3 demonstrates that a methyl hydrogen is within bonding distance of the carbonyl oxygen (3 Å) over a wide range of geometries, not only in the R90 and R270 conformers. Scheffer has established that this distance parameter is the principal determinant of reactivity;^{4,15} so, reaction could conceivably occur from some geometry intermediate between R90 and R270. However, the very low activation energy for triplet decay in otBBP rules out more than slight departures from conformational minima in reaching the transition state. The rectangles mark regions in which the energy is no more than 1.0 kcal/mol above the minimum; all possible reactive geometries thus closely resemble either R90 or R270.

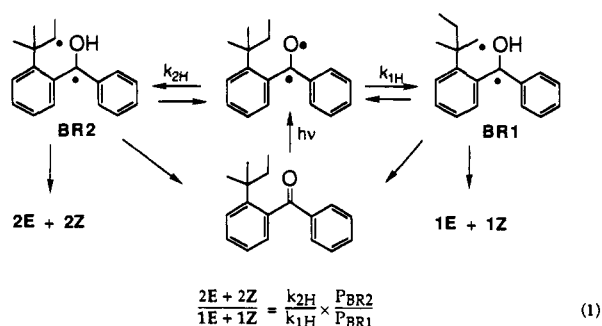
Despite the favorable distances, the methyl hydrogens make angles ω near 90° in both R90 and R270. Moreover, the angle θ is also near 90° in the R90 conformer; it has a more acceptable value of 160° in R270. Computations by Houk and Dorigo on intramolecular hydrogen transfer in flexible chains⁹ have dramatized the importance of θ being near 180° ; the small value of θ attainable in 1,4-hydrogen transfers explains their rarity, while the large value attainable in 1,6-transfers explains their relatively low ΔH^\ddagger values. Consequently, given the high barrier to rotating the methyl group near the carbonyl in R90, theory predicts that reaction at the methyl in this conformation should be slow and should not contribute much to overall triplet decay.

Despite having preferred geometries in which the only close methyl hydrogen is perpendicular (in R270) or nearly perpendicular (in R90) to the plane of the carbonyl n orbital, otAmBP forms indanol photoproducts that represent 20–80% hydrogen abstraction from a “poorly positioned” methyl group. The molecule assumes mainly a R270-like geometry in the crystalline state yet produces 30% combined 1E and 1Z. In solution, the R90 geometry should also be populated; reaction at its ethyl group is impossible, and reaction at a methyl group involves large values of ω and presumably awful values of θ . Nonetheless, significant amounts of reaction always occur at the methyl despite its hydrogens being in poor orientations either for proper C–H–O alignment (R90) or with regard to the half-empty n orbital of the triplet carbonyl (R90 and R270). *It is clear that the “poor” values of ω do not significantly diminish the reactivity of the methyl hydrogens.* This qualitative conclusion must be tempered by the realization that the flexibility of the *tert*-amyl group *a priori* might allow significant “improvement” in ω and θ values at the transition state relative to the reactant and that the reactant is the triplet, not the ground state on which calculations and

(14) Chandler, W. D.; Goodman, L. *J. Mol. Spectrosc.* **1970**, *35*, 232.

(15) Burke has also correlated reactivity with distance in the intramolecular abstraction of hydrogen atoms by alkoxy radicals: Burke, S. D.; Silks, L. A.; Strickland, S. M. S. *Tetrahedron Lett.* **1988**, *29*, 2761.

Scheme 3



spectroscopic measurements were performed. Regarding the latter proviso, it is known that the only significant change in geometry produced by n, π^* excitation is a slight lengthening of the C–O bond.^{14,16} Our calculations reveal no difference in rotational barriers between the triplet and ground state. Regarding the first proviso, there can be little endothermic conformational motion involved in the reaction coordinate, since the measured activation energy for otBBP of only 2.5 kcal/mol and the steric congestion of the reactant allow little leeway.¹⁷ Nonetheless, the transition state may provide better orientation angles than does the ground state.

Biradical Partitioning. In order to determine more quantitatively what these results reveal about orientational preferences, we must convert product ratios into relative rate constants for hydrogen abstraction. Scheme 3 depicts the simple competition that produces the observed product ratios, which are described by eq 1. As in most reactions proceeding through biradicals, product ratios are determined by the product of two separate competitions: the relative rates of formation of the biradicals (k_{2H}/k_{1H}) and the relative partitioning of the biradicals between cyclization and reversion to the ground-state ketone (P_{BR}). We must understand how the P_{BR2}/P_{BR1} ratio can vary in order to correctly deduce k_{2H}/k_{1H} ratios from product ratios.

The P_{BR} values for BR1 and BR2 appear to differ somewhat from the value for the single biradical from otBBP, which is 0.04 in benzene but rises to unity in methanol, where hydrogen bonding suppresses biradical disproportionation back to the ground-state ketone.¹⁸ The low quantum yields for otAmBP and the methanol-induced increase in the yields of 2E and 2Z suggest that BR2 cyclizes less efficiently than does BR1. The flash kinetics observation of two biradicals with different lifetimes supports this conclusion. The fact that 2E and 2Z are more sterically crowded than 1E and 1Z could well alter the relative cyclization rates of the two unsolvated biradicals in competition with disproportionation back to the starting ketone. We return to this point below.

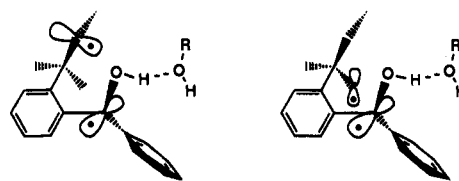
The fact that methanol increases the total cyclization efficiency of otAmBP only to 43% probably means that BR1 and BR2 cannot hydrogen bond to solvent as readily as can the less sterically crowded biradical from otBBP. Unfortunately, with just 43% of the biradicals trapped by methanol, we must rely on an estimate of the BR2/BR1 ratio for the 57% that still revert to ketone. Chart 4 lists several options that would explain the measured product ratios. One extreme possibility is that P_{BR1} is unity in methanol, as it is for otBBP. In that case, P_{BR2} would be only 30% and the 5:1 k_{2H}/k_{1H} value would represent its maximum possible value in solution. However, as option 1 shows, such a high rate ratio would demand the unlikely value of 0.13 for P_{BR1} in benzene, three times higher than that of otBBP. Thus, we conclude that the actual ratio is much closer to the product ratio

(16) The benzoyl group of triplet phenyl ketones maintains planarity.⁵
 (17) Encinas, M. V.; Lissi, E. A.; Lemp, E.; Zanocco, A.; Scaiano, J. C. *J. Am. Chem. Soc.* **1983**, *105*, 1856.
 (18) Wagner, P. J. *J. Am. Chem. Soc.* **1967**, *89*, 5898. Wagner, P. J.; Kochevar, I. E.; Kempainen, A. E. *J. Am. Chem. Soc.* **1972**, *94*, 7489.

Chart 4

	$\frac{\Phi_2}{\Phi_1} = \frac{k_{2H} \times P_{BR2}}{k_{1H} \times P_{BR1}}$	
	OPTION 1 — $P_{BR1} = 1$ in methanol	
in methanol	$\frac{\Phi_2}{\Phi_1} = \frac{0.83 \times 0.30}{0.17 \times 1.0}$	= $\frac{0.26}{0.17}$
in benzene:	$\frac{\Phi_2}{\Phi_1} = \frac{0.83 \times 0.017}{0.17 \times 0.13}$	= $\frac{0.014}{0.020}$
	OPTION 2 — k_{2H}/k_{1H} independent of solvent	
in benzene:	$\frac{\Phi_2}{\Phi_1} = \frac{0.61 \times 0.023}{0.39 \times 0.05}$	= $\frac{0.014}{0.020}$
in methanol	$\frac{\Phi_2}{\Phi_1} = \frac{0.61[0.41 + 0.59 \times 0.023]}{0.39[0.41 + 0.59 \times 0.05]}$	= $\frac{0.26}{0.17}$
	OPTION 3 — $P_{BR1} = P_{BR}$ for otBBP	
in benzene:	$\frac{\Phi_2}{\Phi_1} = \frac{0.50 \times 0.028}{0.50 \times 0.04}$	= $\frac{0.014}{0.020}$
in methanol	$\frac{\Phi_2}{\Phi_1} = \frac{0.61[0.41 + 0.59 \times 0.028]}{0.39[0.41 + 0.59 \times 0.04]}$	= $\frac{0.26}{0.17}$

of 3:2. Partial suppression of disproportionation is common in bulky hydroxy biradicals and is thought to reflect an equilibrium between hydrogen-bonded and free biradicals, with none of the former disproportionating.¹⁹ BR1 and BR2 very likely share a common conformational preference, with the ethyl group perpendicular to the benzene ring, as in the reactant ketone, so that the equilibrium constant for solvation should be similar for both biradicals. In that case, the BR2/BR1 ratio should approximate k_{2H}/k_{1H} for both solvated and free biradicals. If we presume that the quantum yields in methanol reflect solvated biradicals that cyclize with 100% efficiency and free biradicals that cyclize in only 2.3% and 5% efficiency, respectively, the actual quantum yields indicate a k_{2H}/k_{1H} ratio of 1.56, as shown in Chart 4, option 2. The comparable amounts of two biradicals observed by flash kinetics support this estimate. It is important to emphasize that modest variations in unsolvated P_{BR} values cannot alter the fact that ~95% of the reaction in methanol arises from the 40+% solvated biradicals and therefore closely reflects the k_H ratio in that solvent.



The 50:50 product ratios in dioxane and acetonitrile provide an alternative explanation (option 3), namely a 50:50 k_{2H}/k_{1H} ratio in aprotic solvents, with $P_{BR1} = 0.04$ as it is in otBBP. This view requires that hydrogen-abstraction selectivity in methanol be slightly different from that in aprotic solvents, evidence for which is discussed below. *Whichever option is chosen, k_{2H}/k_{1H} is 1.6 in methanol and 1.0–1.6 in aprotic solvents.*

Temperature Effects. In liquid methanol, product ratios do not vary over a 150° temperature range. Either there is no change in the k_{2H}/k_{1H} ratio or any change is exactly compensated for by a reciprocal change in the P_{BR2}/P_{BR1} ratio. Given the normally greater reactivity of secondary relative to primary C–H bonds and the presumably less favorable geometry of the methyl groups in otAmBP, k_{1H} might have had a higher activation energy than k_{2H} . If so, k_{2H}/k_{1H} would have increased with decreasing temperature. The lack of such an effect reinforces our earlier conclusion that the abnormally low activation energy for otBBP

(19) Wagner, P. J.; Kelso, P. A.; Kempainen, A. E.; McGrath, J. M.; Schott, H. N.; Zepp, R. G. *J. Am. Chem. Soc.* **1972**, *94*, 7506.

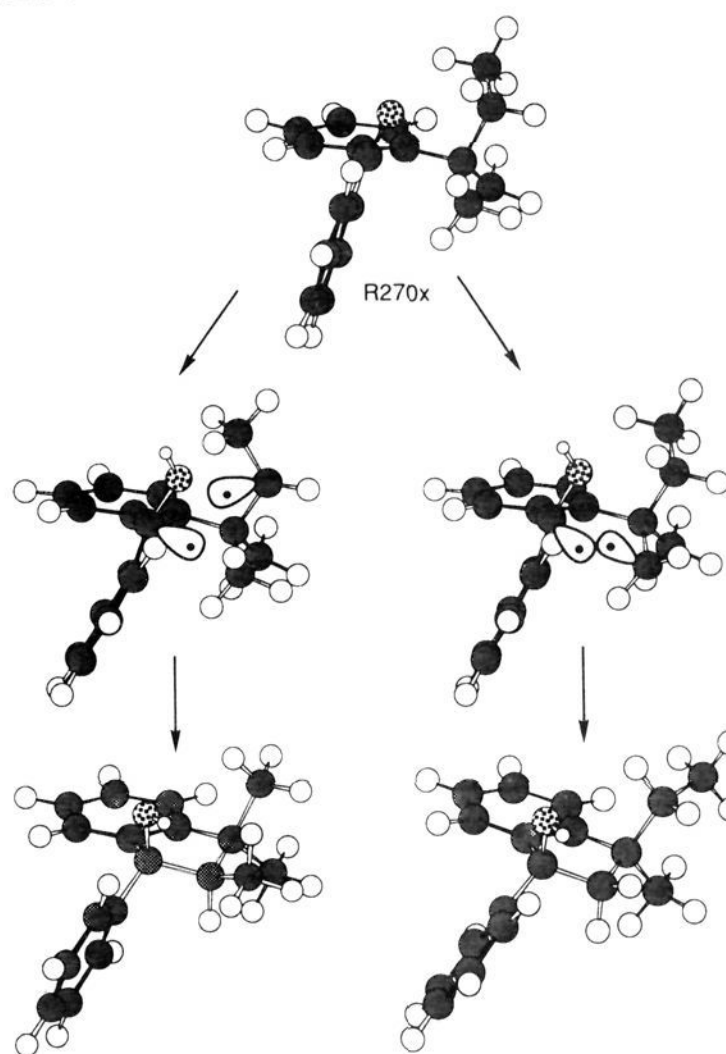
reflects hydrogen abstraction being driven by relief of steric strain more than by intrinsic C–H reactivity.² However, changes in conformational equilibria can affect the *observed* relative rates of hydrogen abstraction.²⁰ For example, if R90, in which only a methyl can react, is slightly lower in energy than R270, then decreasing the temperature would decrease the 2/1 ratio, provided that no change in *P* values also occurs. This exact effect was observed in toluene. Since the various computations suggested comparable energies for R90 and R270, we tentatively suggest that differential solvation may affect conformational populations of *otAmBP*, especially in its triplet state.

Phase Effects. In frozen methanol at 77 K, regioselectivity is nearly identical to that in liquid methanol. Selectivity in the crystal at room temperature is somewhat greater, while reaction on silica gel produces the highest 2/1 selectivity. We cannot easily convert these solid-state product ratios into k_{2H}/k_{1H} values, since there is no way to efficiently trap the biradicals such as can be done in solution. If all the biradicals have similar P_{BR} values, then $k_{H2}/k_{H1} = 2.4$. The possibility that the P_{BR2}/P_{BR1} ratio is significantly lower than unity would lead to a higher k_{H2}/k_{H1} value. If the *tert*-amyl rotation is slow in the solid, then rotation of BR2 into the correct geometry for cyclization may compete even less well with disproportionation back to the ground-state ketone than in solution, where bond rotations are rapid but cyclization is only ~3% efficient. In contrast, BR1 need not rotate before cyclizing, so its partitioning should be independent of environment. The 2-fold difference in biradical lifetimes and the solvent effects on product ratios both suggest different biradical partitioning efficiencies. Fortunately, the phase dependence of diastereoselectivity can provide information about the flexibility of intermediates in the crystal.

Diastereoselectivity. Solvation of hydroxy biradicals by Lewis bases is known to greatly influence the diastereoselectivity of their cyclization. A variety of 1,4- and 1,5-biradicals that show significant preferences for cyclizing with a methyl *trans* rather than *cis* to a phenyl in hydrocarbon solvents shows reduced selectivity in alcohols.^{17,18,21} BR2 is unusual in showing no 2E/2Z selectivity in benzene and only a 1.3 *E/Z* ratio in Lewis bases. BR1 also shows no selectivity in benzene but a significant 1.8 *Z/E* ratio in Lewis base solvents. Apparently, the solvated hydroxyl prefers to be pseudoequatorial slightly more than does a phenyl. These biradicals appear to mimic the behavior of other 1,5-biradicals in that preexisting conformational preferences are more important than steric interactions created by cyclization.²² We assume here that ISC is coupled with cyclization, such that chemical barriers determine product ratios.^{11,20}

In contrast to the situation in solution, biradical cyclization shows appreciable diastereoselectivity in all the solid environments, with a large shift toward 2Z and a smaller shift toward 1Z in the crystal and in an alcohol glass at 77 K. In contrast, reaction on silica gel produces only 2:1 2Z/2E selectivity and no 1Z/1E selectivity. Scheffer has reported several comparisons between excited-state hydrogen abstraction in the solid state and in solution.²³ In most cases, the stereoselectivity of biradical cyclization is enhanced in the solid but does not reach 100%. Observed selectivity always reflects a least-motion picture of biradical cyclization. The general conclusion is that molecular flexibility in the crystal is low enough to reduce but not totally prevent inversion of some radical sites by bond rotations. This picture can be altered to the extent that photochemistry occurs at defect sites. We have eliminated the possibility that the crystal-phase photochemistry of *otAmBP* occurs primarily at somewhat

Scheme 4



disordered surfaces by showing that the same product ratios are produced at different depths into the crystal. Conversions decreased significantly in layers further removed from the surface; this constancy of product ratios in these low-conversion experiments also reduces the possibility of reaction occurring in “melts” caused by product buildup.

The markedly greater diastereoselectivity for cyclization of *otAmBP* in solid environments relative to in solution certainly indicates that most bond rotations are frozen in the solid. Scheme 4 shows that least-motion collapse of both BR2 and BR1, formed from the R270x ketone geometry, produces the two *Z* diastereomers observed to be preferred in solids.

The minor yield of 2E in frozen environments probably indicates that hydrogen transfer causes sufficient disturbance of the solid lattice to allow some rotation of the secondary radical site. The formation of 1E is harder to explain. We pointed out above the possibility that as much as 15% of the molecules may have geometry R30 in the crystal, which places the methyl hydrogens in the positions occupied by H₁ and H₂ in R270. Least-motion cyclization of the resulting biradicals would form both 1Z and 1E, which represents only 8% of the total product in the crystal. Since the *tert*-amyl group becomes asymmetric when one methyl group loses a hydrogen, the only way BR1 formed from R270x can form 1E is for a 180° rotation around the benzene–C(OH)–phenyl bond. Since such a rotation would entail significant disruption of the crystal lattice, the presence of some R30 seems the preferable explanation for formation of 1E in the crystal.

The diminished stereoselectivity on silica presumably reflects the greater flexibility of molecules adsorbed on a surface relative to those packed in a crystal. Since there is *Z/E* selectivity for 2 but not for 1, it is likely that the 1:1 1E/1Z ratio results from comparable populations of R270 and R90. The larger (3.5:1) 2/1 ratio compared to that in the crystal (2.4:1), despite the likelihood that half the molecules are R90 and can form only BR1, suggests that cyclization of BR2 is indeed somewhat hindered in the crystal. If one assumes that half of 1 comes from R90 on silica, one concludes a 7:1 2/1 ratio from R270. One can

(20) (a) Lewis, F. D.; Johnson, R. W.; Johnson, D. E. *J. Am. Chem. Soc.* **1974**, *96*, 6090. (b) Wagner, P. J. *Top. Curr. Chem.* **1976**, *66*, 1.

(21) Wagner, P. J. *Acc. Chem. Res.* **1989**, *22*, 83.

(22) Wagner, P. J.; Park, B.-S. *Tetrahedron Lett.* **1991**, *32*, 165.

(23) Ariel, S.; Evans, S. V.; Garcia-Garibay, M.; Harkness, B. R.; Omkaram, N.; Scheffer, J. R.; Trotter, J. *J. Am. Chem. Soc.* **1989**, *111*, 5591. Lewis, T. J.; Rettig, S. J.; Scheffer, J. R.; Trotter, J.; Wireko, F. *J. Am. Chem. Soc.* **1990**, *112*, 3679.

then conclude that the lower 2/1 ratio in the crystal indicates a P_{BR1}/P_{BR2} ratio of 3 and thus a k_{H2}/k_{H1} ratio of 7.

Conclusions

The measured product ratios from *ot*AmBP, after correction for differential cyclization efficiencies of the two biradicals formed by triplet-state δ -hydrogen abstraction, indicate that significant amounts of reaction take place at a methyl hydrogen oriented at $\omega \approx 90^\circ$ in the ground state. The alternative methylene hydrogen has $\omega \approx 40^\circ$. The estimated k_{H2}/k_{H1} ratio is 1.5 in solution and 7 in the crystal. Conformational flexibility in solution can lower the methyl ω value below 90° , such that $\cos^2 \omega$ has a nonzero value. However, calculated energies and atomic coordinates, when compared to the low measured activation energy for hydrogen abstraction, indicate that the transition state cannot depart much from the conformational minima R270 and R90. Thus, these results provide further evidence that rate constants for hydrogen abstraction by triplet carbonyls are not subject to a very stringent stereoelectronic requirement, at least as regards angle ω . This conclusion refers to the ground-state geometry, not the transition state, which can adopt different angles, especially in flexible molecules. However, the particular attraction of *ot*AmBP is its high steric congestion, which should preclude the low-energy transition state from departing significantly from the reactant geometry. The higher selectivity inferred from the solid-state behavior of *ot*AmBP is thus very important. The maximum estimated k_{H2}/k_{H1} ratio of 7:1, based largely on enhanced diastereoselectivity, reflects the expected low molecular mobility in the crystal. If relative rate constants adhere to the $\cos^2 \omega$ rule^{20b} and if H_2 reacts from $\omega = 40^\circ$, we might conclude that ω for H_1 attains $\sim 73^\circ$. However it does not seem reasonable to associate the much smaller solution selectivity with a H_1 ω value near 40° . Likewise, the small values of θ that accompany H_1 reactivity are theoretically bad but have considerable precedent;⁴ they accentuate the uncertainties that accompany evaluation of orientational requirements in this simplest of chemical reactions.

Experimental Section

Chemicals. Solvents were all purified and distilled prior to use.

Preparation of *ot*AmBP. The strategy reported for *ot*BBP²⁴ was followed, with some updated methods. A mixture of 34 mL of nitric acid and 44 mL of sulfuric acid was added dropwise over 1 h to 54 g of *tert*-amylbenzene (Columbia). An ice bath kept the temperature $\sim 50^\circ\text{C}$. After neutralization and workup, the product mixture was fractionally distilled to separate the lower boiling ortho isomer from *p*-nitro-*tert*-amylbenzene, of which 64 g was obtained as a yellow liquid: bp 164–66 $^\circ\text{C}$ (13 Torr); $^1\text{H NMR}$ (CDCl_3) δ 0.68 (t, $J = 7.5$ Hz), 1.33 (s), 1.69 (quar, $J = 7.5$ Hz), 7.48 (d), 8.15 (d); MS m/e 193, 164 (base), 136, 117, 106, 91, 77, 43.

Bromine (17.4 mL) was added dropwise over 30 min to a stirred mixture of the nitro compound, 56.5 g of silver sulfate, 300 mL of concentrated sulfuric acid, and 33 mL of water at ambient temperature.²⁵ After 3 h, the solution was poured into 1 L of dilute sodium sulfite. The AgBr was filtered off and the filtrate extracted into ether. Normal workup and fractional distillation provided 84 g of 2-bromo-4-nitro-*tert*-amylbenzene as a yellow oil: bp 153–58 $^\circ\text{C}$ (1 Torr); $^1\text{H NMR}$ (CDCl_3) δ 0.45 (t), 1.30 (s), 1.90 (quar), 7.35 (d), 7.90 (dd), 8.25 (d); MS m/e 216, 214, 194, 164 (base), 115, 91, 77, 43, 39.

The bromo-nitro compound (17 g) as a solution in 120 mL of 95% ethanol and 15 mL of concentrated HCl was reduced in a Parr hydrogenator in the presence of 0.15 g of amorphous Pt(IV) O_2 (Aldrich Adam's catalyst) and at 87–96 psi hydrogen and room temperature. After 10 h, the solution was filtered through Celite; evaporation of the filtrate provided 18 g of the hydrochloride of 3-bromo-4-*tert*-amylaniline. The yellow salt could be recrystallized from a hot benzene/toluene/ethanol mixture, but some decomposition occurred: $^1\text{H NMR}$ (CDCl_3) δ 0.44 (t), 1.30 (s), 1.88 (quar), 7.15–7.60 (m, 3 H).

The hydrochloride salt was partially dissolved in 70 mL of ice-water containing 32 mL of concentrated HCl, to which was added 2.8 g of

sodium nitrile in 6 mL of water. After being stirred at 0°C for 10 min, the suspension was filtered. The clear yellow filtrate was added to 70 mL of ice-cold hypophosphorous acid in an open flask; the mixture was kept in a freezer for 48 h. Ether extraction and workup provided a light brown oil which was vacuum distilled to yield 5.9 g of *o*-bromo-*tert*-amylbenzene: mp 71–72 $^\circ\text{C}$ (1 Torr); $^1\text{H NMR}$ (CDCl_3) δ 0.64 (t), 1.45 (s), 2.03 (quar), 6.95–7.60 (m, 4 H); MS m/e 228, 226, 199, 197, 171, 169, 115, 91, 71 (base), 63, 51, 39.

In flame-dried glassware under argon, 5.8 g of *o*-bromo-*tert*-amylbenzene in 40 mL of freshly dried ether was added dropwise to 1.25 g of Mg turnings in 20 mL of anhydrous ether. Reaction was initiated with a reacting mixture of 1,2-dibromoethane and magnesium in ether; the solution was then refluxed for 4.5 h. A solution of 8 g of benzoyl chloride in 25 mL of ether was added to the cooled Grignard reagent; the mixture was refluxed for 11 h. Neutralization and workup provided an oil that was vacuum distilled, bp 132–134 $^\circ\text{C}$ (1 Torr), to yield 4.65 g of *ot*AmBP as a wet solid. It was purified by column chromatography on silica gel using first pure hexane and then hexane with 2% ethyl acetate. Slow room-temperature recrystallization from mixed hexanes produced white needles, mp 66.5–67.0 $^\circ\text{C}$; IR (CCl_4) 1675 cm^{-1} ; $^1\text{H NMR}$ (CDCl_3) δ 0.68 (t, $J = 7.5$ Hz, 3 H), 1.26 (s, 6 H), 1.69 (quar, $J = 7.5$ Hz, 2 H), 7.04 (dd, $J = 7.5, 1.5$ Hz, 1 H), 7.20 (td, $J = 7.5, 1.0$ Hz, 1 H), 7.38 (td, $J = 7.5, 1.6$ Hz, 1 H), 7.42 (t, $J = 7.5$ Hz, 2 H), 7.485 (br d, $J = 7.5$ Hz, 1 H), 7.56 (tt, $J = 7.5, 1.0$ Hz, 1 H), 7.83 (dd, $J = 7.5, 1.6$ Hz, 2 H); $^{13}\text{C NMR}$ (CDCl_3) δ 9.315, 29.70, 36.71, 39.695, 124.64, 127.82, 128.29, 128.37, 128.80, 130.38, 133.17, 137.82, 139.16, 146.62, 200.10; MS m/z 252, 237, 223, 209, 175, 115, 105, 91, 77 (base), 41, 43, 39.

For X-ray analysis, crystals were grown from *n*-hexane in the refrigerator. Polarized light was used to verify that the crystals were not agglomerates. An appropriate one was sealed in a glass capillary tube.

Spectroscopy. Routine NMR spectra were measured on a Varian Gemini 300 spectrometer. Low-temperature studies of *ot*AmBP were performed on a Varian VMX300 machine: samples in toluene- d_6 , from ambient down to -88°C , and samples in CD_2Cl_2 , from ambient down to -95°C . Product identification was done on VMX300 and VMX500 spectrometers.

Analysis of Photoproducts. *o*-*tert*-Amylbenzophenone (25–50 mg) in 50 mL of benzene was irradiated in an immersion well to 100% conversion, as judged by GC or HPLC, with a Pyrex-filtered medium-pressure mercury arc. Removal of solvent after 100% conversion left a liquid mixture with a parent MS peak at m/z 252. Products were isolated by semipreparative HPLC and a fraction collector, with 3% ethyl acetate in hexane as eluent. For analysis purposes, a 4.6- \times 250-mm silica column was used with a flow rate of 1 mL/min and for separation, a 10- \times 250-mm silica column with a flow rate of 5 mL/min. Four isomeric indanols, each containing small amounts of its diastereomer and indene, were isolated. IR spectra of the individual indanols in CCl_4 showed sharp OH peaks at 3602–3607 cm^{-1} .

(E)-2,3,3-Trimethyl-1-phenylindan-1-ol (2E): $^1\text{H NMR}$ (CDCl_3) δ 0.82 (3 H, d, $J = 7.3$ Hz, 2-Me), 0.89 (3 H, s, 3-Me), 1.36 (3 H, s, 3-Me), 2.41 (1 H, quar, $J = 7.3$ Hz, 2-H), 7.09 (2 H, distorted d), 7.2–7.45 (7 H, m); irradiation at δ 0.82 produced the following NOE enhancements δ 1.36 2.5%, δ 2.4 2.5%, δ 7.3–7.5 3.7%; $^{13}\text{C NMR}$ (CDCl_3) δ 10.52, 24.08, 29.24, 43.96, 58.39, 86.66, 122.62, 124.49, 127.05, 127.34, 127.98, 128.79, 144.30, 146.20, 152.09, 157.0.

(Z)-2,3,3-Trimethyl-1-phenylindan-1-ol (2Z): $^1\text{H NMR}$ (CDCl_3) δ 1.01 (3 H, d, $J = 7.3$ Hz, 2-Me), 1.30 (3 H, s, 3-Me), 1.39 (3 H, s, 3-Me), 2.22 (1 H, quar, $J = 7.3$ Hz, 2-H), 6.98 (1 H, d), 7.2–7.5 (8 H, m); irradiation at δ 1.01 produced 4.5% and 2.5% NOE enhancements at δ 2.22 and 1.39, respectively.

(E)-3-Methyl-3-ethyl-1-phenylindan-1-ol (1E): $^1\text{H NMR}$ (CDCl_3) δ 0.96 (3 H, t, $J = 7.4$ Hz), 1.27 (3 H, s), 1.80 (1 H, quar, $J = 7.4$ Hz), 2.29, 2.56 (2 H, AB quar, $J = 14.1$ Hz), 7.07 (1 H, d), 7.2–7.5 (8 H, m).

(Z)-3-Methyl-3-ethyl-1-phenylindan-1-ol (1Z): $^1\text{H NMR}$ (CDCl_3) δ 0.81 (3 H, t, $J = 7.4$ Hz), 1.42 (3 H, s), 1.58–1.72 (1 H, complex m), 2.26, 2.45 (2 H, AB quar, $J = 14.1$ Hz), 7.01 (1 H, d), 7.2–7.5 (8 H, m). A mixture of the *Z* and *E* isomers was irradiated at δ 1.27; NOE enhancements were measured at δ 1.80 (1.7%), 2.29 (1.9%), and 7.07 (2.9%). Irradiation of the same mixture at δ 1.42 produced NOE enhancements at δ 2.26 (0.8%), 2.56 (0.9%), and 7.0 (0.8%).

The isolated indanols contained small amounts of the two dehydration products and were forced to completely dehydrate by treatment with HCl, although merely standing in CDCl_3 for a day was equally effective: 1-phenyl-2,3,3-trimethylindene $^1\text{H NMR}$ (CDCl_3) δ 1.30 (s, 6 H), 1.96 (s, 3 H), 7.1–7.5 (m, 9 H); 1-phenyl-3-methyl-3-ethylidene $^1\text{H NMR}$

(24) Smith, P. A. S.; Antoniadis, E. P. *Tetrahedron* 1960, 9, 210.

(25) Crawford, M.; Stewart, F. H. C. *J. Chem. Soc.* 1952, 4443.

(CDCl₃) δ 0.69 (t, $J = 7.4$ Hz, 3 H), 1.37 (s, 3 H), 1.78, 1.89 (AB quar of quar, $J = 13.5, 7.4$ Hz, 2 H), 2 H), 6.46 (s, 1 H), 7.2–7.5 (m, 7 H), 7.58 (d, $J = 6.9$ Hz, 2 H). A mixture of the two indenenes gave a parent MS peak at m/z 234.

Samples of 0.01 M in several deuterated solvents were irradiated to complete conversion in NMR tubes attached to an immersion well; the ratios of integrated product NMR signals were used to calibrate the HPLC analyses of indanols. Such a sample in benzene-*d*₆ produced the following characteristic proton resonances (500 MHz): **2Z** δ 0.94 (d, $J = 7.3$ Hz, 2-Me), 1.16 (s, 3-Me), 1.20 (s, 3-Me), 2.10 (quar, $J = 7.3$ Hz, 2-H); **2E** δ 0.72 (d, $J = 7.3$ Hz, 2-Me), 0.80 (s, 3-Me), 1.14 (s, 3-Me), 2.20 (quar, $J = 7.3$ Hz, 2-H); **1Z** δ 0.66 (t, $J = 7.4$ Hz, 3-Et), 1.32 (s, 3-Me), 1.462, 1.505 (AB quar of quar, $J = 14, 7.4$ Hz, Et CH₂), 2.18, 2.34 (AB quar, $J = 14$ Hz, ring CH₂); **1E** δ 0.80 (t, $J = 7.4$ Hz, 3-Et), 1.08 (s, 3-Me), 1.610, 1.662 (quar of quar, $J = 7.4, 14$ Hz, Et CH₂), 2.14, 2.44 (AB quar, $J = 14$ Hz). Only trace amounts of indenenes were present in such samples.

Solid-State Irradiation. A single crystal was irradiated in a capillary tube inside a sealed test tube that was fastened to an immersion well. After irradiation, the sample was quickly extracted with a few successive drops of appropriate solvents. For irradiation in silica gel, the ketone was dissolved in methylene chloride with 200 mesh silica gel. After the solvent was evaporated under low pressure, the resulting sample of doped silica gel was packed into a melting point capillary tube. This sample was irradiated by attaching it to an immersion well. The irradiated capillary tube containing a sample was broken into pieces, and the organics were extracted into a deuterated solvent for NMR analysis followed by HPLC analysis. For irradiation on silica gel, the ketone was dissolved in a slurry of 200 mesh silica gel in methylene chloride. The dried silica was then placed in a capillary tube and irradiated as for the crystal.

Quantitative Procedures. Quantum yields were measured on 0.1 M otAmBP solutions that had been degassed and sealed. Samples in methanol were irradiated in parallel with 0.1 M valerophenone in benzene actinometers and samples in benzene, with 0.1 M *o*-methylvalerophenone in benzene actinometers. Indanol product yields were determined by HPLC analysis; they were converted to quantum yields by measurement of acetophenone yields from the two actinometers, for which the reported values are 0.33¹⁷ and 0.016,¹³ respectively.

Flash kinetics studies were performed on deaerated ketone samples

~0.005 M in methanol using nitrogen laser excitation and a standard apparatus.²⁶ Biradical transient absorption was monitored at 370 nm.

Computations. MMX calculations were performed with PCModel.²⁷ Energies were minimized at 10° increments for rotation around the benzene-*tert*-amyl bond. MM2 and AM1 energy minimizations were performed on a Cache-Tektronix workstation, with a similar dihedral drive.

X-ray crystallography was performed on a 0.2- \times 0.4- \times 0.7-mm crystal with Mo K α radiation ($\lambda = 0.71073$ Å) on a Nicolet P3F diffractometer. The orthorhombic (space group *Pbca*) cell parameters are $a = 12.92(2)$ Å; $b = 13.96(2)$ Å; $c = 16.20(2)$ Å; $V = 2921(5)$ Å³; $Z = 8$; $\rho = 1.15$ g/cm³. Data were collected at 204 K using the θ - 2θ scan technique. A total of 1116 reflections were collected, of which 921 were unique and not systematically absent. Lorentz-polarization and anisotropic decay corrections were applied to the data. The structure was solved by the direct-methods program SHELXS-86²⁸ with full-matrix least-squares refinement. Positional parameters are presented in the supplementary material.

Acknowledgment. This work was supported by NSF Grants CHE85-06703, CHE88-15052, and CHE91-20931. The NMR spectrometers used for product analysis were partially funded by NSF Grant CHE88-00770 and NIH Grant RR047550. X-ray equipment was purchased with the help of NSF Grant CHE84-003823. We thank Dr. Tito Scaiano (University of Ottawa) and the NRCC in Ottawa for their hospitality and cooperation in the measurement of biradical lifetimes.

Supplementary Material Available: Tables of crystallographic positional and thermal parameters (2 pages); a table of observed and calculated structure factors (11 pages). This material is contained in many libraries on microfiche, immediately follows this article in the microfilm version of the journal, and can be ordered from the ACS; see any current masthead page for ordering information.

(26) Scaiano, J. C. *J. Am. Chem. Soc.* **1980**, *102*, 7747.

(27) Serena Software, Bloomington, IN.

(28) Sheldrick, G. M. In *Crystallographic Computing 3*; Sheldrick, G. M., Kruger, C., Goddard, R., Eds.; Oxford University Press: Oxford, 1985; pp 175–189.